- 7 Supplementary Figures + legends.
- 6 Supplementary Tables

(starts next page)

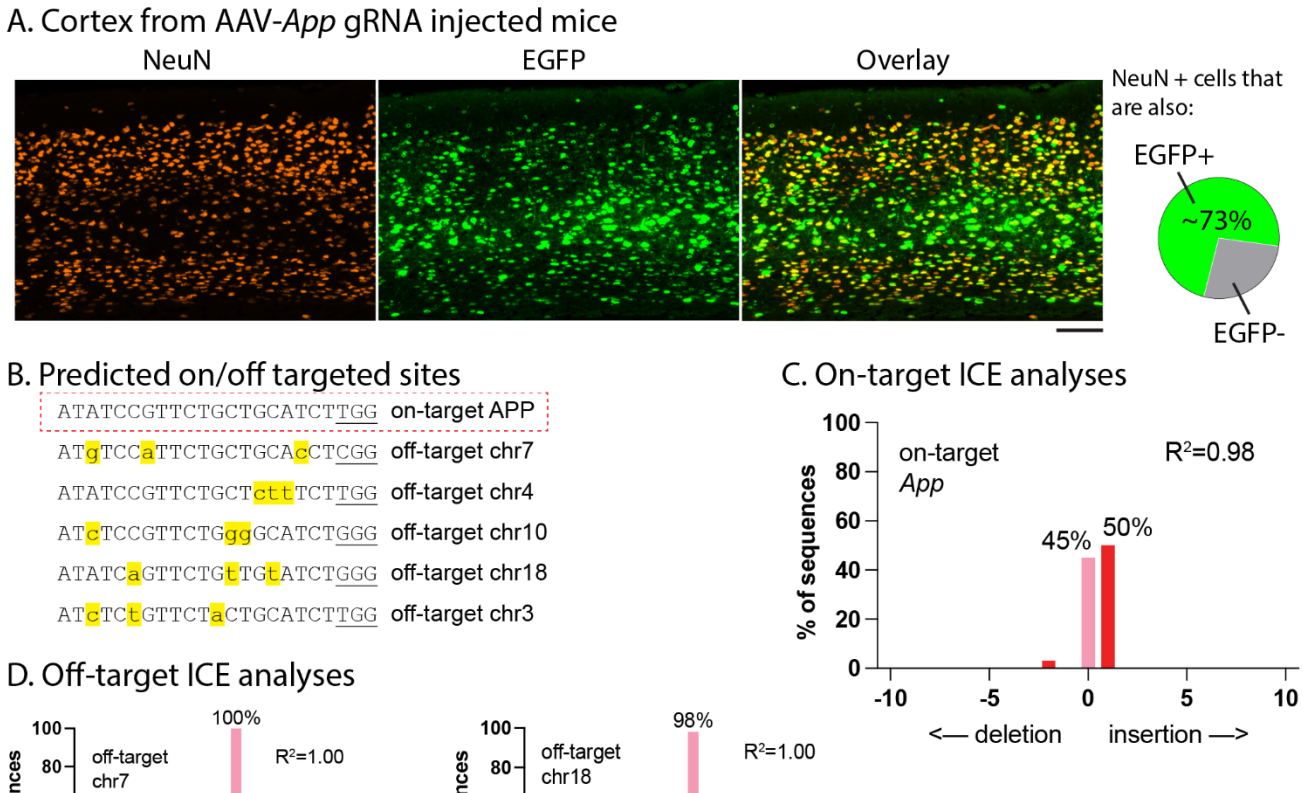

Supplementary Figure 1: Further characterization of histology and genomics (related to main Fig. 1).

A) Sections from one-year old mouse brains (SpCas9-KI) injected with AAV-PHP.eb-*App*-gRNA (EGFP-tagged), and two-color immunostained for NeuN (neuronal nuclei) and EGFP to determine fraction of transduced neurons. Pie chart on right shows the mean number of neurons that were transduced (N = 3 mice per condition, 8 cortical regions and ~ 1000 neurons were analyzed from each animal). These results are consistent with previously published estimates using the AAV-PHP.eb capsid. Scale bar = 100 mm

B) Alignment of on-target *App* gRNA site (top row, dashed red box) with predicted off-target sites contain ≤ 3 mismatches (using Cas-OFFinder). All PAM sites are underlined, and nucleotide mismatches in the off-target sites are highlighted in yellow/lowercase.

C, D) On-target **(C)** and off-target **(D)** Interference of CRISPR Edits (ICE) analysis of DNA from cortices from *App*-KI/SpCas9-KI mice AAV-injected with *App*-gRNA. Data plotted as frequency of predicted editing outcome (size of insertion or deletion as a percentage to total sequences). Correlation with expected variant percentages (R^2) are noted. Note the extremely low frequency of detectable edits within predicted off-target sites.

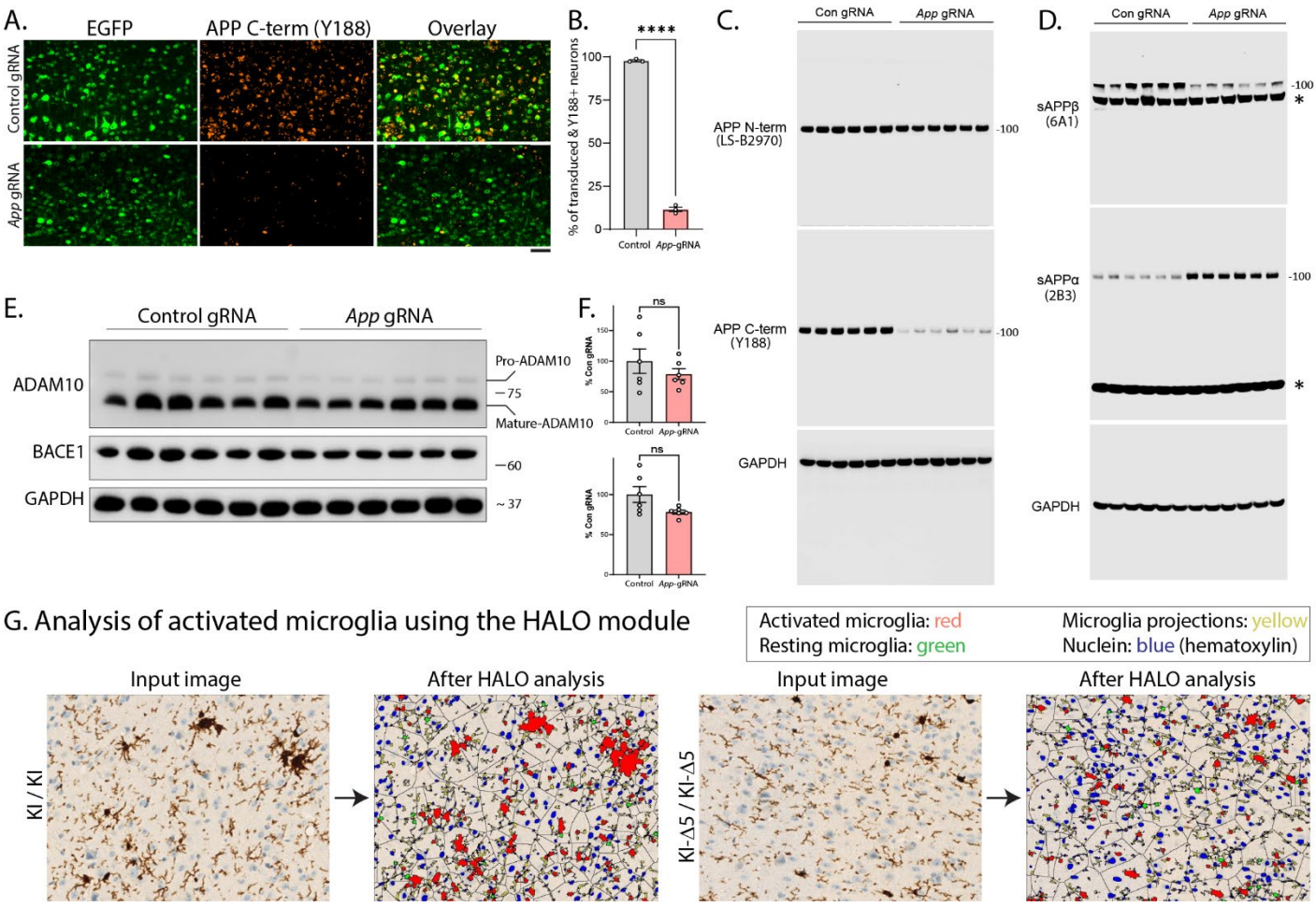

<u>Supplementary Figure 2</u>: Further characterization ad analyses of AAV-driven *in vivo* CRISPR editing (related to main Figs. 1/2).

A) Sections from one-year old SpCas9-KI mouse brains injected with AAV-PHP.eb-*App*-gRNA (EGFP-tagged) or scrambled-gRNA control, and stained for EGFP and Y188 (APP C-terminus antibody) to determine fraction of transduced neurons that also lacked the APP C-terminus; quantified in **B)**. Data shown as mean +/- SEM percentage of EGFP positive neurons that also showed Y188 staining (N = 3 mice per condition, (seven cortical areas were sampled, and >1000 cells were analyzed from each mouse). Note that a large fraction of *App*-gRNA transduced neurons lacked Y188 staining. Scale bar = 50 mm.

C, D) Full gels from **Figures 1 H)** and **1 I)**, asterisk (*) marks non-specific bands.

E, F) One-year old SpCas9-KI mice were injected with AAVs carrying *App*-gRNA or scrambled-gRNA control, and brains were immunoblotted for APP secretases ADAM10 and BACE1; quantified in **F)**. Data shown as mean +/- SEM, expressed as a percentage of control-gRNA injected group (N = 6 mice for each condition, ns = non-significant). Note that there are no significant changes in the levels of secretases after *App* C-terminus editing.

G) Automated detection of activated microglia by HALO module software in *App*-KI and *App* -KI-Δ5 tissue sections stained for Iba-1.

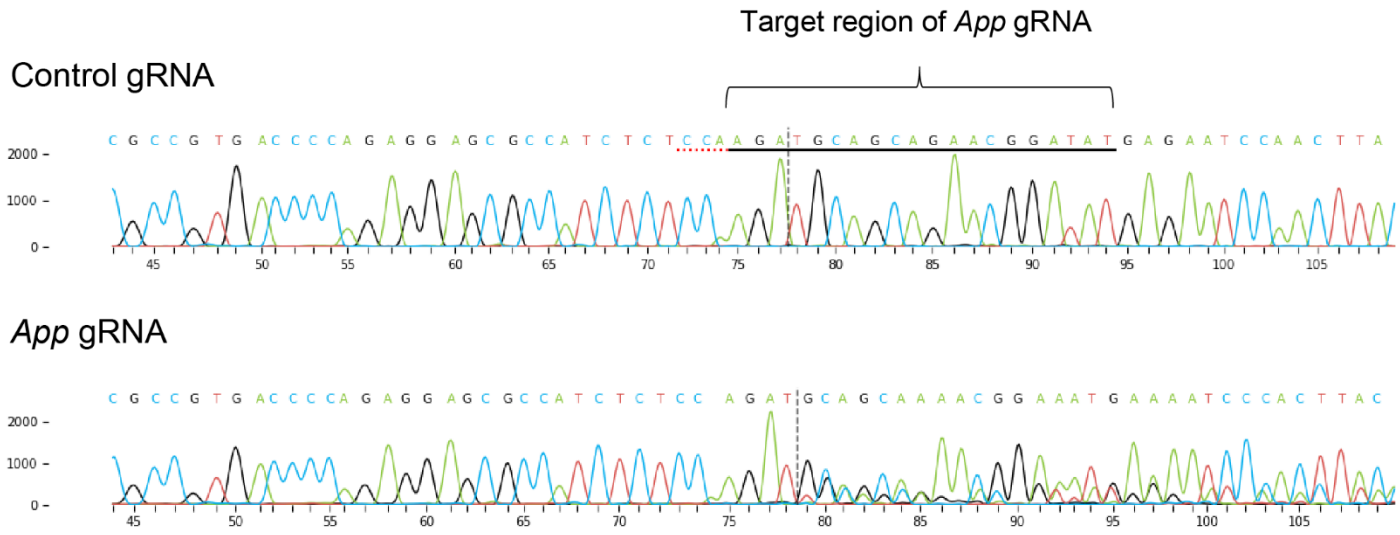

<u>Supplementary Figure 3</u>: Confirmation of *App*-editing in hippocampal slices used for LTP analyses (related to main Fig. 2).

Sanger sequencing confirmation of editing in slices used for LTP experiments. Primers flanking the target site of the *App* gRNA (labeled in the figure) were designed, and amplicons were produced from the genomic DNA of tissue slices. These amplicons were sequenced to confirm CRISPR-editing. Note nucleotide-mismatch within targeted *App*-gRNA loci, that is seen only in AAV-*App*-gRNA injected brains.

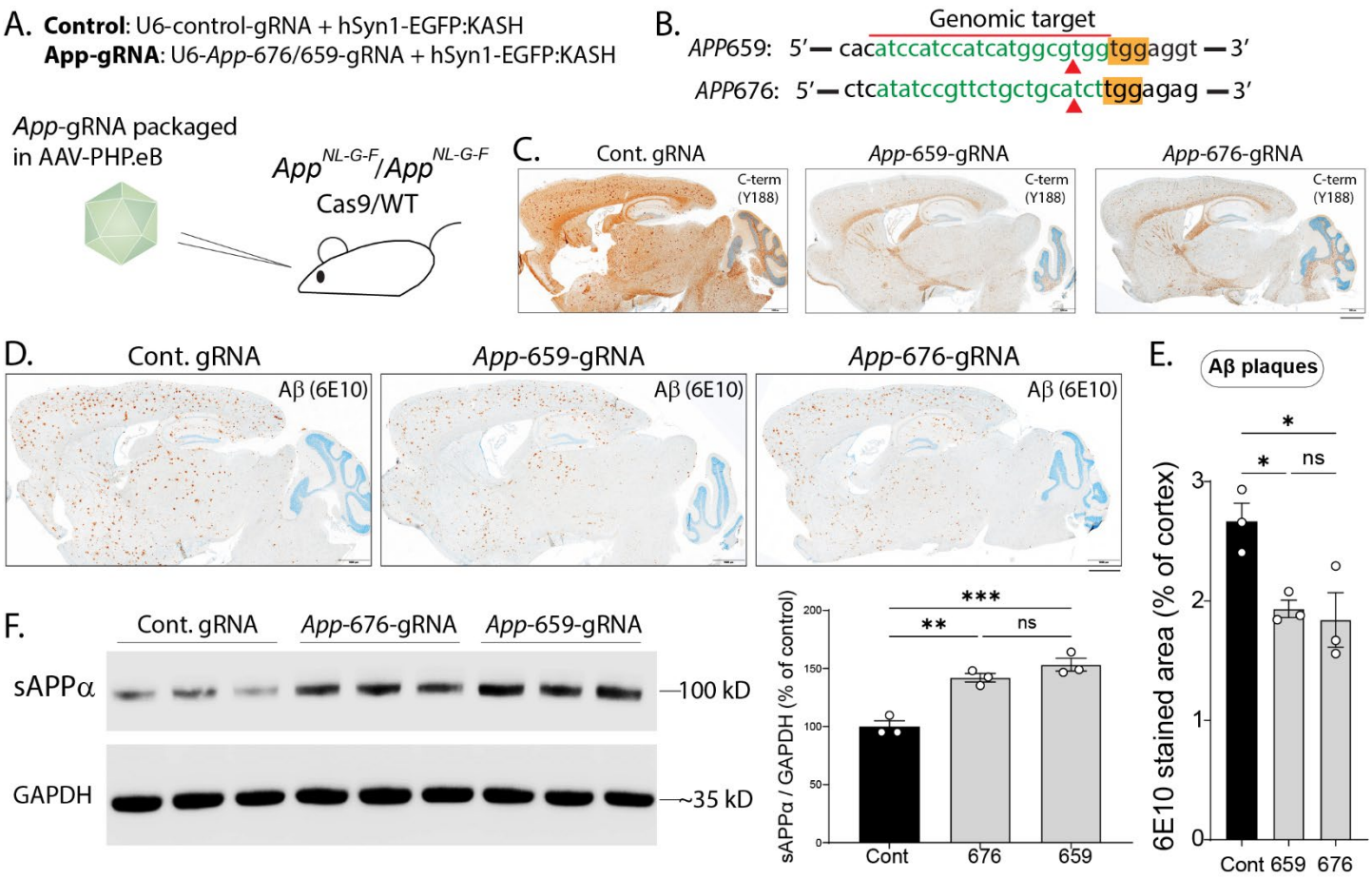

Supplementary Figure 4: Comparison of *App*-659 and *App*-676 gRNA (related to main Figs. 2/3).

A) Experimental design to inject AAV-*App*-659/676 gRNA by intravenous injection in App-KI/Cas9-KI mice.

B) Genomic targets and predicted cut-sites (red arrowheads) in App for 659/676gRNAs, PAM sites highlighted yellow.

C) Staining of the extreme APP C-terminus (Y188 antibody) in control and 659/676-gRNA injected mouse brains. Note attenuated staining in *App*-gRNA injected brains, indicating C-terminal truncation of protein.

D-E) Attenuated Aβ deposition in 659/676-gRNA injected mouse brains.

F) Western blots from mouse brains to examine sAPPα shows an increase in 659/676-gRNA injected mouse brains.

All data shown as mean +/- SEM, expressed as a percentage of control. N = 3 mice/group, *p <0.01, **p <0.001, ***p <0.0001, ns = non-significant.

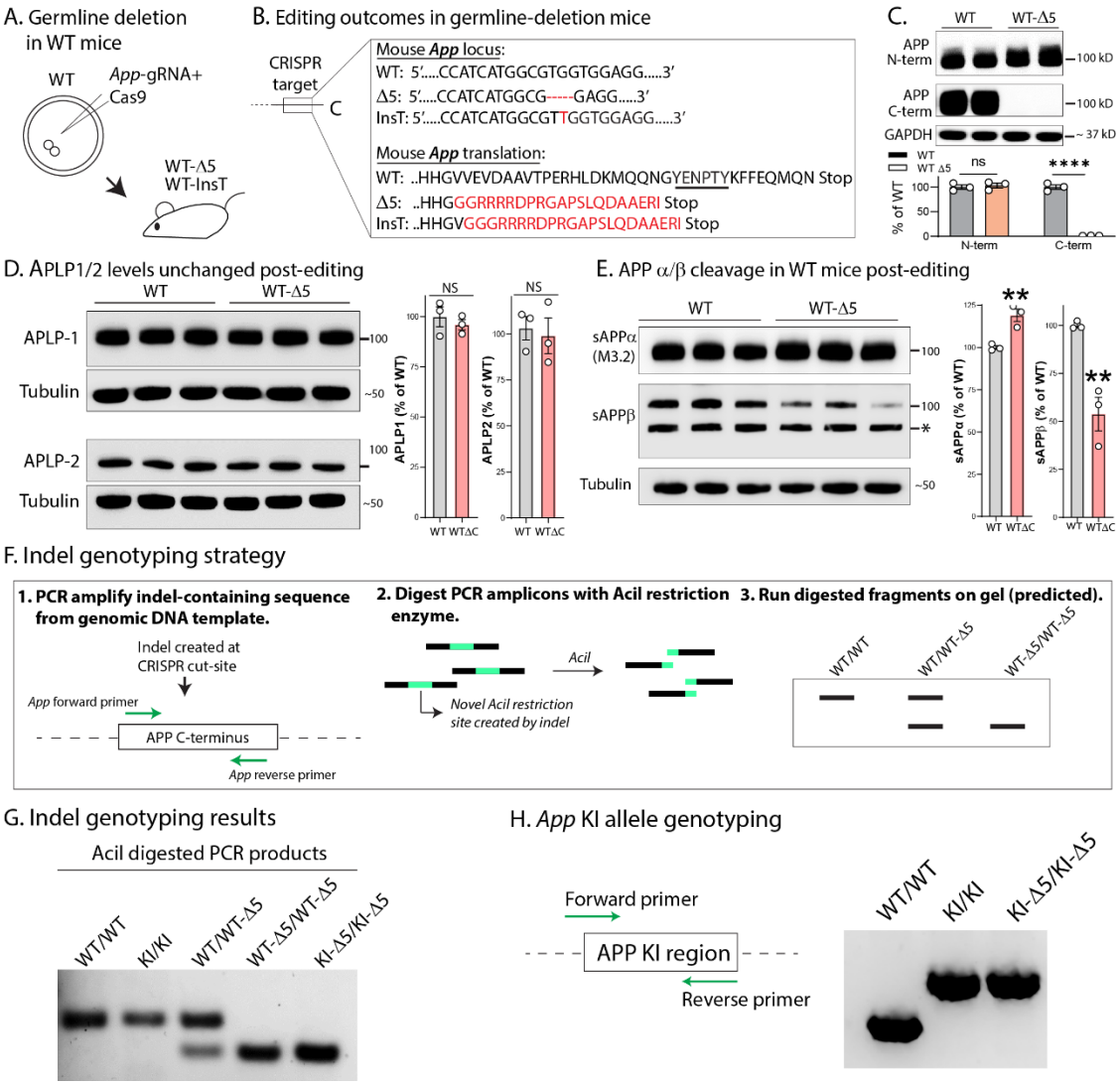

<u>Supplementary Figure 5</u>: Further characterization of *App*-KI and *App*-KID5/InsT mouse brains (related to main Fig. 3).

A) Zygotes from WT mice were injected with *App*-gRNA/Cas9 ribonucleoprotein complexes targeting the *App* C-terminus, and resulting founders were screened and outbred to produce stable heterozygous and homozygous lines.

B) Two edited strains with effective deletion of the last ~35 amino acids were selected. Schematic and sequences show the edited mouse *App* loci and expected translational products. Note that one strain has deletion of 5 amino acids (D5), and the other has a single amino-acid insertion (Insert-T) that lead to indels and premature stop codons.

C) Western blots of edited WT mouse brains using antibodies to APP N- and C-terminus. Note that the C-terminus Y188 antibody is unable to recognize APP, while signal from the N-terminus antibody is intact.

D) Western blots for APLP1 and APLP2 levels (APP homologues) in cortical/hippocampal lysates from WT and WT-Δ5 mice; quantified on right. Data expressed as mean +/- SEM, expressed as a percentage of WT. N = 3 mice per condition, NS = non-significant.

E) Western blots for sAPPα and sAPPβ in cortical/hippocampal lysates from WT and WT-Δ5 mice. Asterisk (*) indicates a non-specific band. Data shown as mean +/- SEM, expressed as a percentage of WT. N = 3 mice/group, **p <0.001.

F) Genotyping strategy to identify Δ5bp indel in *App* genomic deletion mice. Deletion of the 5bp generates a novel restriction-site that was digested by the restriction-enzyme AciI, allowing us to identify the genomically

deleted mice. Specifically, indel-containing sequences were PCR-amplified, digested with AciI, and the digested fragments were run on agarose gels to identify genomically deleted animals.
G) DNA gel of PCR products from WT and *App*-KI mice after digestion with AciI. Note that genomic deletion of the *App* C-terminus (right 3 lanes) generates a cleavage product that runs as a lower band.
H) Genotyping to confirm retention of the *App* knock-in allele in KI-Δ5bp mice. Note that presence of the *App*-KI allele leads to an upper band, allowing identification of KI animals.

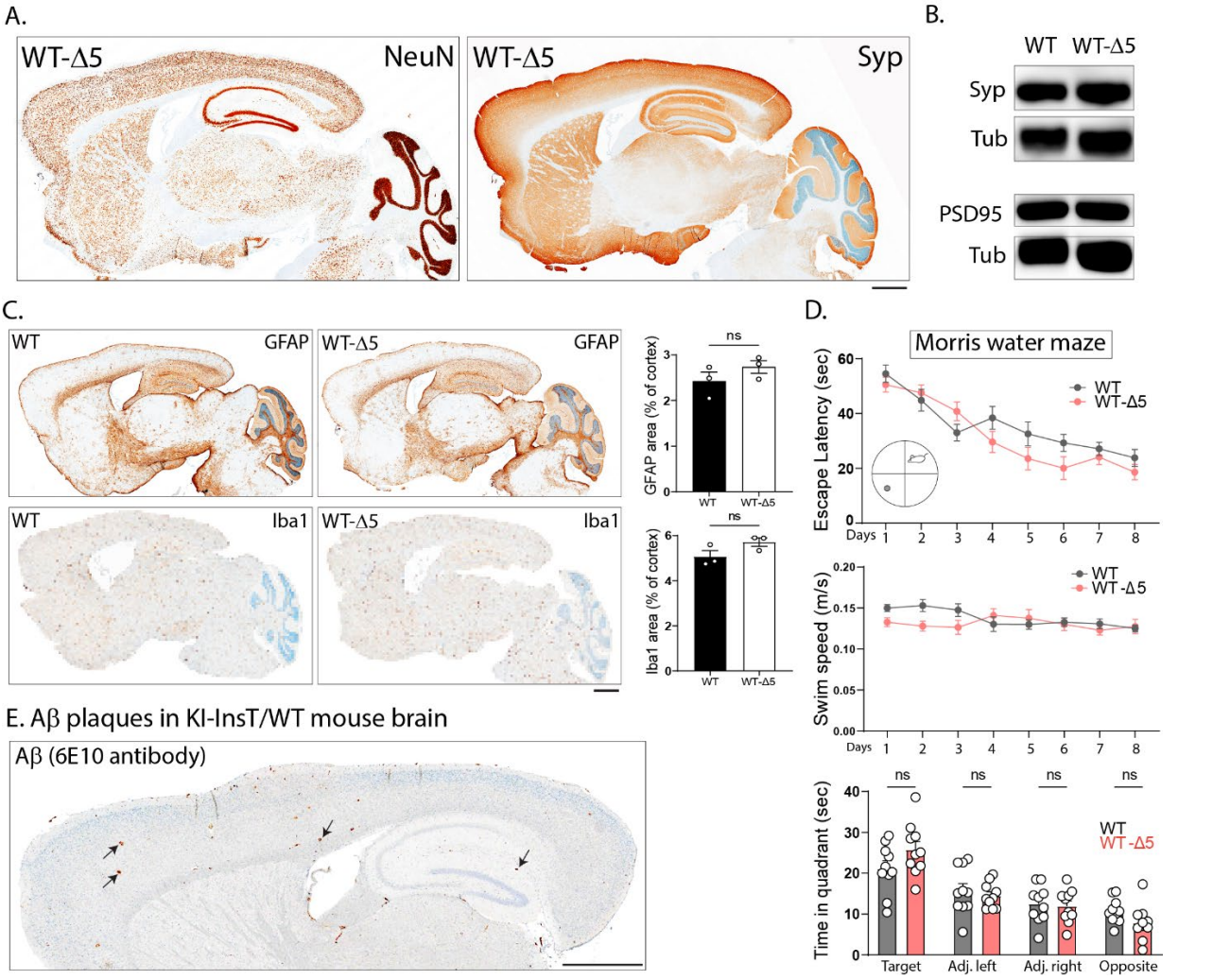

<u>Supplementary Figure 6</u>: Safety evaluation of *App*-editing in WT mice (related to main Fig. 3).
A) Neuronal (NeuN) and synaptic (synaptophysin) staining in the WT germline-edited mice (*App*-D5, a strain that effectively lacks the YENPTY-motif). Note that the brains appear grossly normal. Immunoblots of pre- and post-synaptic markers in **B)**. Scale bar = 1mm.
C) Comparison of astrocytes and microglia show no significant changes in the WT germline-edited mouse brains, compared to WT controls; quantified on right. Scale bar = 1mm.
D) Morris water maze test for memory does not show any deficits in WT germline-edited mouse brains, compared to WT controls (escape latency – top, swim speed – middle, probe-trial results – bottom).
E) Representative image of Aβ (6E10) staining in *App*-KI-InsT/WT heterozygous mice lacking the last ~ 35 amino acids of APP. Note that plaques are rarely seen in this setting (few marked with small arrows). Quantification of Aβ in these mice is shown in **Figure 3C** Scale bars = 1mm, data are shown as mean +/- SEM. N = 3/condition for **C)**, and 10/condition for **D)**, ns = non-significant.

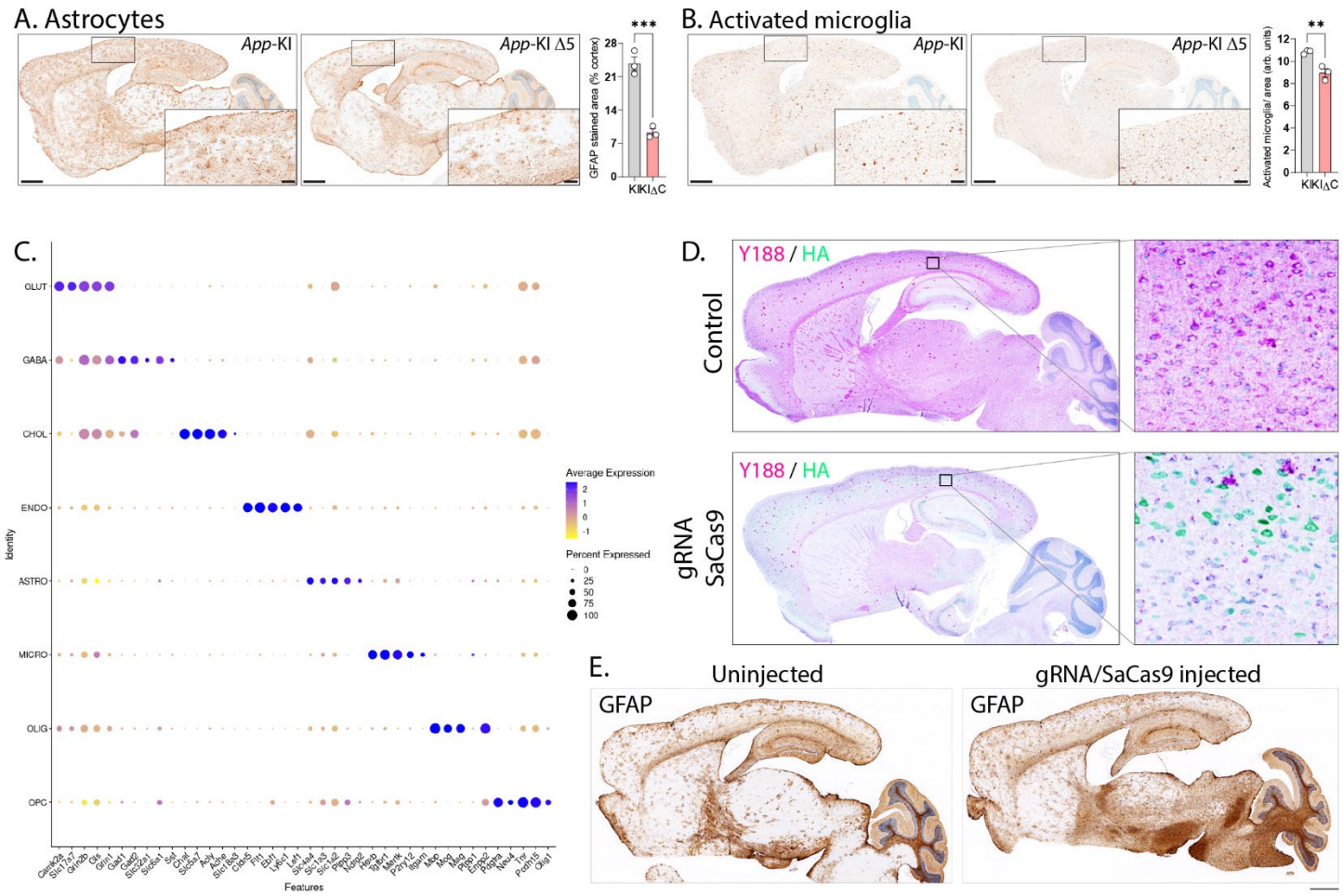

<u>Supplementary Figure 7</u>: Dot-plots for cell signatures relevant for sNucSeq experiments (related to main Fig. 3).

A, B) Representative histologic sections showing that astrocytic and microglial activation in *App*-KI mice (homozygous) is ameliorated by germline editing of the *App* C-terminus; staining quantified on right (N=3animals per condition, mean +/- SEM, ** p <0.01, *** p <0.001). Scale bars: main = 1 mm, zoomed inset = 200 mm.

C) Dot-plot representation of marker gene-expression for the cell types that were identified. The size of the dot represents the percentage of nuclei in the cluster expressing the marker gene, and the color indicates the expression level relative to the average expression across all nuclei (the data is scaled such that the average expression across all nuclei = 0). Yellow indicates lower than average expression; a graduated shift in color from yellow to purple to dark blue indicates increasing levels of expression with dark blue indicating the highest level of expression. Note that expression of marker genes is largely restricted to the appropriate cell-types, indicating successful cell-type clustering and identification of cell-types.

D) Representative sections of AAV-*App*-gRNA/SaCas9 injected brains double-stained with anti-HA and anti-APP-C-terminus (Y188) antibodies. Note strong Y188-staining (magenta) in un-injected brains, but attenuation in *App*-gRNA/SaCas9 injected brains. Zoomed insets on right highlight selective diminution of Y188-signal in neurons expressing HA (green, marking transduced cells). Scale bars: main = 1 mm, zoomed inset = 100 mm.

E) GFAP staining shows astrocytosis in AAV- *App*-gRNA/SaCas9 injected brains compared to non-injected brains, likely due to immune responses to AAVs.